Original Article

The influence of arm positions on mechanical dyssynchrony measured by gated myocardial perfusion imaging

Zhongqiang Zhao[1#], Cheng Wang[1#], Zeyu Peng[1], Ju Bu[1], Chunxiang Li[1], Dianfu Li[1], Weihua Zhou[2], Rongsheng Lu[3], Lijun Tang[4], Yong Li[1,5]

[1]Department of Cardiology, The First Affiliated Hospital of Nanjing Medical University, Nanjing, China; [2]Department of Applied Computing, Michigan Technological University, Houghton, MI, USA; [3]Jiangsu Key Laboratory for Design and Manufacture of Micro-Nano Biomedical Instruments, Southeast University, Nanjing, China; [4]Department of Nuclear Medicine, The First Affiliated Hospital of Nanjing Medical University, Nanjing, China; [5]Department of Cardiology, The People's Hospital of Qijiang District, Chongqing, China

Contributions: (I) Conception and design: R Lu, L Tang, Y Li; (II) Administrative support: D Li, W Zhou; (III) Provision of study materials or patients: Z Peng, J Bu, C Li; (IV) Collection and assembly of data: Z Zhao, C Wang; (V) Data analysis and interpretation: Z Zhao, C Wang; (VI) Manuscript writing: All authors; (VII) Final approval of manuscript: All authors.

[#]These authors contributed equally to this work.

Correspondence to: Yong Li, MD. Department of Cardiology, The First Affiliated Hospital of Nanjing Medical University, 300 Guangzhou Road, Nanjing 210029, China. Email: liyongmydream@126.com; Lijun Tang, MD. Department of Nuclear Medicine, The First Affiliated Hospital of Nanjing Medical University, 300 Guangzhou Road, Nanjing 210029, China. Email: tanglijun@njmu.edu.cn; Rongsheng Lu, PhD. Jiangsu Key Laboratory for Design and Manufacture of Micro-Nano Biomedical Instruments, Southeast University, Southeast University Road 2#, Nanjing 214135, China. Email: lurs@seu.edu.cn.

Background: In routine procedures, patient's arms are positioned above their heads to avoid potential attenuation artifacts and reduced image quality during gated myocardial perfusion imaging (G-MPI). However, it is difficult to achieve this action in the acute period following pacemaker implantation. This study aimed to explore the influence of arm positioning on myocardial perfusion imaging (MPI) in different types of heart disease.

Methods: This study was conducted retrospectively. A total of 123 patients were enrolled and underwent resting G-MPI using a standard protocol with arms positioned above their heads and again with their arms at their sides. All individuals were divided into 3 groups: the normal group, the obstructive coronary artery disease (O-CAD) group, and the dilated cardiomyopathy (DCM) group. The G-MPI data were measured by QGS software and Emory Reconstruction Toolbox, including left ventricular ejection fraction (LVEF), end-diastolic volume (EDV), end-systolic volume (ESV), extent, total perfusion deficit (TPD), summed rest score (SRS), scar burden, phase standard deviation (SD), and phase histogram bandwidth (BW).

Results: In total, extent, TPD, EDV, ESV, LVEF, systolic SD, systolic BW, diastolic SD, and diastolic BW were all significantly different between the 2 arm positions (all $P<0.01$). On the Bland-Altman analysis, both EDV and ESV with the arm-down position were significantly underestimated ($P<0.001$). Meanwhile, TPD, extent, and LVEF with the arm-down position were significantly overestimated ($P<0.05$). Systolic SD, systolic BW, diastolic SD, and diastolic BW were systematically overestimated ($P<0.001$). In the DCM group (n=52), EDV, ESV, systolic SD, systolic BW, diastolic SD, and diastolic BW were identified as significantly different by the paired *t*-test between the 2 arm positions ($P<0.05$). In the O-CAD group (n=32), scar burden, ESV, LVEF, and diastolic BW were significantly different between the 2 arm positions ($P<0.05$).

Conclusions: Systolic and diastolic dyssynchrony parameters and most left ventricular (LV) functional parameters were significantly influenced by arm position in both normal individuals and patients with heart failure (HF) with different pathophysiologies. More attention should be given to LV dyssynchrony data during clinical evaluation of cardiac resynchronization therapy (CRT) implantation procedure.

Keywords: Gated myocardial perfusion imaging (G-MPI); left ventricular mechanical dyssynchrony (LVMD); phase analysis; heart failure (HF)

Submitted Dec 19, 2022. Accepted for publication Aug 30, 2023. Published online Sep 22, 2023.
doi: 10.21037/qims-22-1404
View this article at: https://dx.doi.org/10.21037/qims-22-1404

Introduction

Gated myocardial perfusion imaging (G-MPI) is a widely used, noninvasive, and cost-effective method of imaging that plays an important role in diagnosing, evaluating prognosis, evaluating the viability, and assessing the effectiveness of therapy in heart disease (1). A recent study found that left ventricular mechanical dyssynchrony (LVMD) was more highly correlated with cardiovascular disease (CVD) and all-cause mortality than electrical dyssynchrony (2). Meanwhile, the myocardial perfusion imaging (MPI) phase analysis showed some advantages over other imaging methods with wide availability and excellent reproducibility in valuing global left ventricular (LV) dyssynchrony, such as phase standard deviation (SD), phase histogram bandwidth (BW), and phase entropy (PE). In recent years, nuclear image-guided approaches for cardiac resynchronization therapy (CRT) have shown significant clinical value in assessing LV myocardial viability and mechanical dyssynchrony, recommending the optimal LV lead position, and navigating the LV leading to the target coronary venous site.

Quality control of G-MPI data is a key point to acquiring valid results. However, attenuation artifacts are common in the anterior, inferior, and lateral myocardium, which results in lower diagnostic accuracy. Anterior attenuation has been linked with breast artifacts, whereas inferior attenuation is associated with diaphragm or subdiaphragmatic interference (3). Lateral attenuation and reduced image quality have been related to the left arm during image acquisition. Therefore, MPI is acquired with the left arm positioned above the patient's head in routine procedures (4). However, in the acute period, pacemaker implantation for CRT makes it difficult to achieve such positioning. Additionally, some elderly patients are not able to complete studies in this position. Although new MPI technology has improved the image resolution and quality (5), little data have been obtained about the impact of arm positioning on LV parameters and mechanical dyssynchrony. Therefore, we aimed to explore the influence of arm positioning on MPI in different types of heart disease. We present this article in accordance with the STROBE reporting checklist (available at https://qims.amegroups.com/article/view/10.21037/qims-22-1404/rc).

Methods

Patient population

This study was conducted retrospectively. This study consecutively enrolled 123 individuals at the First Affiliated Nanjing Medical University Hospital from December 2018 to August 2020. All individuals were divided into 3 groups with the aim to achieve representativeness of the general population: a normal group, an obstructive coronary artery disease (O-CAD) group, and a dilated cardiomyopathy (DCM) group. O-CAD was defined as coronary artery stenosis greater than 50% by coronary angiography or dual-source computed tomography (CT) in at least 1 of the main coronary arteries, previous history of coronary revascularization, or myocardial infarction (6). DCM was diagnosed with the patient's history and exclusion of other etiological factors that might cause heart failure (HF), with LV ejection fraction (LVEF) <45% according to the recent criteria (7). The other individuals were divided into the normal group with the following exclusion criteria: hypertension, diabetes, smoking, hyperlipidemia, other high cardiovascular risk factors, severe arrhythmia, postoperative percutaneous coronary intervention (PCI), HF, and myocardial perfusion abnormalities. This study was approved by the Institutional Ethical Committee of the First Affiliated Hospital of Nanjing Medical University, and informed consent was obtained from all individuals. This study conformed to the provisions of the Declaration of Helsinki (as revised in 2013).

Single-photon emission CT (SPECT) MPI assessment

All individuals underwent resting electrocardiogram (ECG)-SPECT MPI with their arms positioned above their heads and again with their arms at their sides. MPI was performed approximately 60 minutes after injection using 740–1,110 MBq of 99mTc-sestamibi. The SPECT images

were acquired in a dual-headed camera (CardioMD; Philips Medical Systems, Eindhoven, Netherlands) with a standard protocol with a 20% energy window of approximately 140 KeV, 180° orbit, 32 steps with 25 seconds per step, 8-bin gating, and 64 planar projections per gate. After MPI data acquisition was completed, reconstruction processing was performed using QPS/QGS software to obtain short-axis, vertical long-axis, and horizontal long-axis tomographic images and then obtain left cardiac function parameters, including LVEF, end-diastolic volume (EDV), end-systolic volume (ESV), total perfusion deficit (TPD), extent, summed rest score (SRS), and scar burden.

Meanwhile, image reconstruction and reorientation were performed by Emory Reconstruction Toolbox (ERToolbox; Atlanta, GA, USA) for mechanical dyssynchrony, including phase distribution of LV systolic dyssynchrony (LVSD) and LV diastolic dyssynchrony (LVDD). The MPI images were reconstructed by ordered subset expectation maximization (OSEM) with 3 iterations and 10 subsets and then filtered by a Butterworth low-pass filter with an order of 10 subsets and a cutoff frequency of 0.3 cycles/cm.

The resulting gated short-axis MPI images were sent to an interactive tool for automatized access to LV contour parameters by an automatic myocardial sampling algorithm that searched 3-dimensionally (3D) for the maximal count circumferential profiles in each cardiac frame. Subsequently, the onset of mechanical contraction and relaxation throughout the cardiac cycle were obtained based on multi-harmonic Fourier approximations (8). Then, the LVMD was represented by the phase distribution of LVSD and LVDD for the entire left ventricle, and quantitative parameters of LVMD were calculated as the SD and BW, respectively (8,9).

Statistical analysis

Continuous variables were expressed as the mean ± standard deviation, and categorical variables were expressed as numbers and percentages. Comparisons between arms-up and arms-down were performed using Student's *t*-test for paired data. One-way analysis of variance (ANOVA) was performed for continuous variables, including baseline characteristics and LV parameters. Pearson's correlation analysis was applied to assess the association between arms up and arms down in left cardiac parameters. The Bland-Altman analysis of agreement was used to compare the average absolute difference in LV measurements between the 2 groups (10). Additionally, the Kruskal-Wallis H-test was employed to assess the differences in baseline characteristics among the 3 groups, which encompassed variables such as hypertension, diabetes, body mass index (BMI), alcohol consumption, and smoking (11). A 2-tailed P<0.05 was considered statistically significant. Statistical analysis was performed with the software SPSS 22.0 (IBM Corp., Armonk, NY, USA).

Results

A total of 123 individuals who underwent SPECT MPI were included in this study (*Figure 1*). The baseline characteristics of high cardiovascular risk factors are listed in *Table 1* including age, gender, hypertension, diabetes, BMI, smoking, and alcohol consumption. Besides, in O-CAD patients, there were 24 cases of stable angina and 8 cases of myocardial infarction. For all individuals, the age was 61.27±10.87 years, and 74.80% (n=92) of patients were male. There were statistically significant differences in age, hypertension, BMI, alcohol consumption, and smoking between the normal group, O-CAD group, and DCM group (all P<0.05) (*Table 1*). In total, Pearson's correlation analysis revealed that there were high correlations for SRS, extent, scar burden, TPD, EDV, ESV, LVEF, systolic SD, systolic BW, diastolic SD, and diastolic BW between the arm-up and arm-down positions in all variables (all P<0.01, *Table 2*). *Figure 2* and *Figure 3* illustrate the G-MPI obtained from a normal individual (58-year-old male, 63 kg, BMI 23.9 kg/m^2). A noticeable finding in the images is that the perfusion in the inferior-lateral and inferior walls appears to be decreased in the images with the arms down when compared to the images with the arms up. However, apart from SRS and scar burden, several parameters including extent, TPD, LVEF systolic SD, systolic BW, diastolic SD, and diastolic BW exhibited significantly higher values in the arm-down position group compared to the arm-up position group, as determined by the paired *t*-test (all P<0.05) (*Table 2*). Conversely, the arm-down position group showed significantly lower values for EDV and ESV compared to the arm-up position group, as determined by the paired *t*-test. Additionally, in both the arm-up and arm-down position groups, the cardiac function parameters were higher in males compared to females except for LVEF values, as indicated in *Table 3*.

In the Bland-Altman analysis (*Figure 4*), both EDV and ESV with the arm-down position were significantly underestimated by a mean of 5.0 (P<0.001) and 7.5 (P<0.001), respectively, compared with EDV and ESV with the arm-up position. Meanwhile, LVEF, extent, scar burden, and TPD with the arm-down

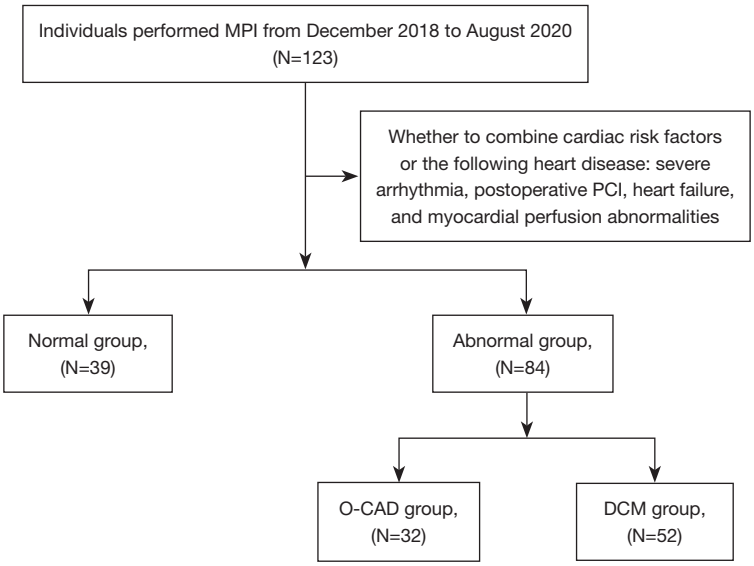

Figure 1 Study flow diagram. MPI, myocardial perfusion imaging; PCI, percutaneous coronary intervention; O-CAD, the obstructive coronary artery disease; DCM, dilated cardiomyopathy.

Table 1 Baseline characteristics of the enrolled patients

Variables	All (n=123)	DCM group (n=52)	O-CAD group (n=32)	Normal group (n=39)	P value
Age (years)	61.27±10.87	62.46±11.14	64.13±11.14	57.10±11.47	0.013
Male	92	40	28	24	0.179
Hypertension	42	22	20	0	<0.001
Diabetes	8	4	4	0	0.059
BMI (kg/m^2)	24.14±2.60	23.32±2.97	25.51±1.71	24.28±1.83	0.025
Smoking	28	16	12	0	<0.001
Alcohol	12	8	4	0	<0.001

Data are expressed as mean ± standard deviation or number. DCM, dilated cardiomyopathy; O-CAD, obstructive coronary artery disease; BMI, body mass index.

position were overestimated compared with those with the arm-up position by a mean of 2.3 (P<0.001), 0.8 (P=0.02), 0.6 (P=0.27), and 1.0 (P=0.005), respectively (*Figures 5*,*6*). Furthermore, to analyze the influence of arm position on LV phase analysis parameters, we examined the difference between BW and SD in both LV systolic and diastolic parameters (*Table 2*). There was a high correlation for systolic SD, systolic BW, diastolic SD, and diastolic BW between the arm-up and arm-down positions in all 3 groups (all P<0.01). Moreover, systolic SD, systolic BW, diastolic SD, and diastolic BW were all higher in the arm-down positions (all P<0.05). Meanwhile, as suggested by the Bland-Altman plot in *Figure 7* and *Figure 8*, systolic SD, systolic BW, diastolic SD, and diastolic BW were systematically overestimated by a mean of 5.6 (P<0.001), 24.1 (P<0.001), 7.4 (P<0.001), and 22.6 (P<0.001), respectively.

In the subgroup of normal individuals (n=39, *Table 4*), SRS, extent, TPD, ESV, LVEF, systolic SD, systolic BW, and diastolic SD were shown to be significantly different by the paired *t*-test between the 2 arm positions (all P<0.05). However, there were no differences in scar burden, diastolic BW, and EDV in the normal group (all P>0.05). In the DCM group (n=52, *Table 5*), EDV, ESV, systolic SD, systolic BW, diastolic SD, and diastolic BW were shown to be significantly different by the paired *t*-test between the

Table 2 Left ventricular functional parameters and the correlations in all groups (n=123) with two arm positions

Variables	Arm-down position	Arm-up position	R value	P value
SRS	5.98±7.28	6.04±7.80	0.928	0.805
Extent	10.15±10.77	8.80±12.05	0.950	0.023
Scar burden	19.82±10.32	9.33±12.30	0.871	0.340
TPD	8.63±8.55	7.65±9.75	0.952	0.001
EDV (mL)	157.57±104.57	162.95±112.58	0.990	0.001
ESV (mL)	93.59±99.45	101.31±109.47	0.986	<0.001
LVEF (%)	52.76±25.83	50.50±24.97	0.978	<0.001
Systolic SD	34.37±19.03	28.76±17.43	0.705	<0.001
Systolic BW	144.33±86.13	120.47±84.21	0.725	<0.001
Diastolic SD	60.67±16.33	53.58±20.04	0.425	<0.001
Diastolic BW	199.67±66.25	177.91±67.80	0.504	<0.001

R values (correlation coefficient), indicate a statistically significant relationship (P<0.01) between the 2 arm positions in all variables. Data are expressed as mean ± standard deviation. SRS, summed rest score; TPD, total perfusion deficit; EDV, end-diastolic volume; ESV, end-systolic volume; LVEF, left ventricular ejection fraction; SD, phase standard deviation; BW, phase histogram bandwidth.

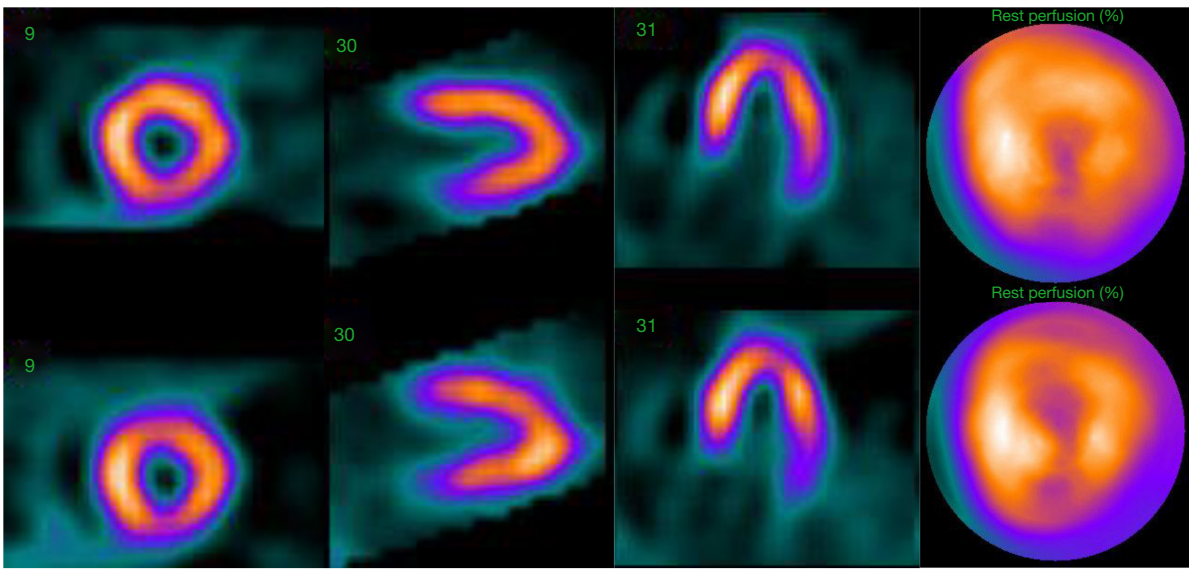

Figure 2 A G-MPI obtained from a normal individual (58-year-old male, 63 kg, BMI 23.9 kg/m^2). The top row represents the images captured with the arms up, while the bottom row shows the images obtained with the arms down. From left to right, the images correspond to the short axis, vertical axis, horizontal axis, and a parametric bull's eye plot. A noticeable finding in the images is that the perfusion in the inferior-lateral and inferior walls appears to be decreased in the images with the arms down when compared to the images with the arms up. G-MPI, gated myocardial perfusion imaging; BMI, body mass index.

2 arm positions (P<0.05). In the O-CAD group (n=32, *Table 6*), scar burden, ESV, LVEF, and diastolic BW were shown to be significantly different by the paired *t*-test between the 2 arm positions (P<0.05).

Discussion

This study investigated the influence of arm position on LVMD parameters in normal individuals and HF patients

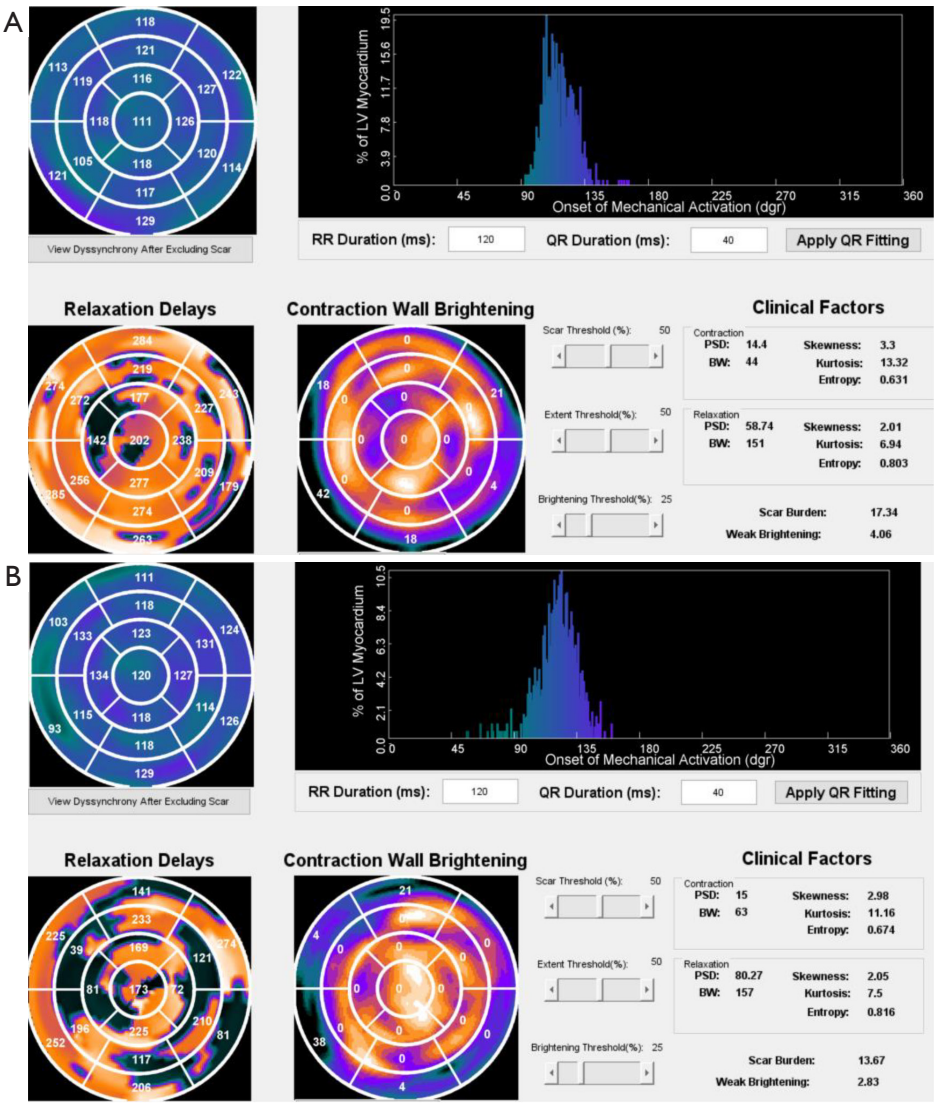

Figure 3 In this normal individual, systolic SD, systolic BW, diastolic SD and diastolic BW were different by the paired *t*-test in arms up (A) compared with arms down (B) (systolic SD: 14.4 *vs.* 15.0; systolic BW: 44.0 *vs.* 63.0; diastolic SD: 58.74 *vs.* 80.27; diastolic BW: 151.0 *vs.* 157.0). SD, phase standard deviation; BW, phase histogram bandwidth.

with different pathophysiologies. The main finding was that systolic and diastolic dyssynchrony parameters and most LV function and perfusion parameters were significantly influenced by arm position in both normal individuals and HF patients with different pathophysiologies.

Gated SPECT (G-SPECT) has been widely used in evaluating the clinical outcome of heart disease and the CRT response. Quantitative analysis of G-SPECT images is becoming an increasingly common tool in the field of nuclear cardiology. Therefore, quality control in acquiring gated MPI data is very important to achieve valid results (12). The Cedars-Sinai QGS program and Emory cardiac toolbox (13), which are commonly used commercially available MPI analysis software packages, can produce reliable computations of LV perfusion and function parameters from G-SPECT MPI data.

However, some potential artifacts and pitfalls should also be paid close attention to. LV segmentation, including precise assignment of LV contours by determining the endocardial and epicardial surfaces, is essential for MPI SPECT quantification. The presence of extracardiac activity can also cause inaccuracy by including adjacent

Table 3 Left ventricular functional parameters in male and female (n=123) with both arm-up and arm-down positions

Variables	Male	Female	P value
SRS			
Arm down	6.24±7.93	5.19±4.90	0.491
Arm up	6.76±8.60	3.90±4.17	0.078
Extent			
Arm down	11.67±11.63	5.65±5.77	0.007
Arm up	11.11±13.51	5.65±5.77	0.005
Scar burden			
Arm down	21.43±11.27	16.72±7.00	0.031
Arm up	21.48±12.55	14.62±5.06	0.004
TPD			
Arm down	9.89±9.24	4.87±4.43	0.004
Arm up	9.03±10.73	3.55±3.74	0.006
EDV (mL)			
Arm down	166.67±107.60	130.55±91.31	0.096
Arm up	172.96±116.54	133.26±95.54	0.090
ESV (mL)			
Arm down	100.79±102.27	72.23±88.68	0.168
Arm up	109.80±114.18	76.10±91.16	0.139
LVEF (%)			
Arm down	51.00±25.45	57.97±26.67	0.195
Arm up	48.54±24.87	56.32±24.76	0.134
Systolic SD			
Arm down	36.73±19.86	27.34±14.44	0.017
Arm up	31.08±18.46	21.89±11.71	0.011
Systolic BW			
Arm down	154.08±88.50	115.39±72.48	0.030
Arm up	133.15±89.32	82.84±51.78	0.004
Diastolic SD			
Arm down	62.36±15.82	55.65±17.04	0.047
Arm up	55.61±20.62	47.54±17.11	0.052
Diastolic BW			
Arm down	208.75±64.39	172.71±65.34	0.008
Arm up	187.67±69.40	148.94±54.07	0.005

Data are expressed as mean ± standard deviation. SRS, summed rest score; TPD, total perfusion deficit; EDV, end-diastolic volume; ESV, end-systolic volume; LVEF, left ventricular ejection fraction; SD, phase standard deviation; BW, phase histogram bandwidth.

extracardiac activity in the LV boundary due to activity related to subdiaphragmatic organs, including the liver and bowel. Besides, weight, BMI, chest circumference, breast attenuation, and bra cup size are better parameters to predict count rate loss, which relates to the quantification of cardiac perfusion and MPI parameters (3,14). A reasonable speculation is that left arm positioning influences the uptake of regional myocardial technetium-99m MPI. Then, the LV boundary region of interest (ROI) was changed according to the location of the maximum pixel count, leading to the inappropriate determination of the point of normalization. However, the current attenuation correction method in the QPS software can effectively compensate for attenuation using the normal limits database. Nonetheless, clinicians may not pay close attention to the subtle variations between patients with their arms up and arms down, as this difference is only present in a small subset of patients. The standard protocol of SPECT is positioning the arms up to maintain the best image quality. Nevertheless, patients with fractures or dislocations of their shoulders or arms may not be able to elevate their arms, especially in patients with pacemaker implantation for CRT during the acute period (15). In a previous study, Toma *et al.* reported that arm positioning did not influence regional myocardial distribution on technetium-99m sestamibi MPI (4). However, Prvulovich *et al.* found that arm positioning influences reconstructed tomographic images depicting regional 201Tl distribution, particularly anterolaterally (16). The different findings in the 2 studies could be explained by the insensitivity of cardiac emission data to truncation, and attenuation correction was not performed in all studies. Furthermore, using a large field of view (FOV) gamma camera might have reduced truncation artifacts in their study. In our study, the normal patients showed higher SRS, extent, and TPD, especially in the lateral wall and anterior lateral wall, which could be explained by the lower uptake of regional myocardial technetium-99m MPI.

Phase analysis provides a new tool to assess LVMD without any additional radiation dose to the patients (17). Mechanical dyssynchrony can be widely present in HF patients, as observed in our research (18). Our previous study and the literature have shown that LVMD is an independent predictor of cardiac complications in patients with DCM and coronary artery disease (19,20). Furthermore, phase analysis can help in identifying potential candidates for CRT, and a study has shown that assessment of mechanical left ventricular dysfunction (LVD)

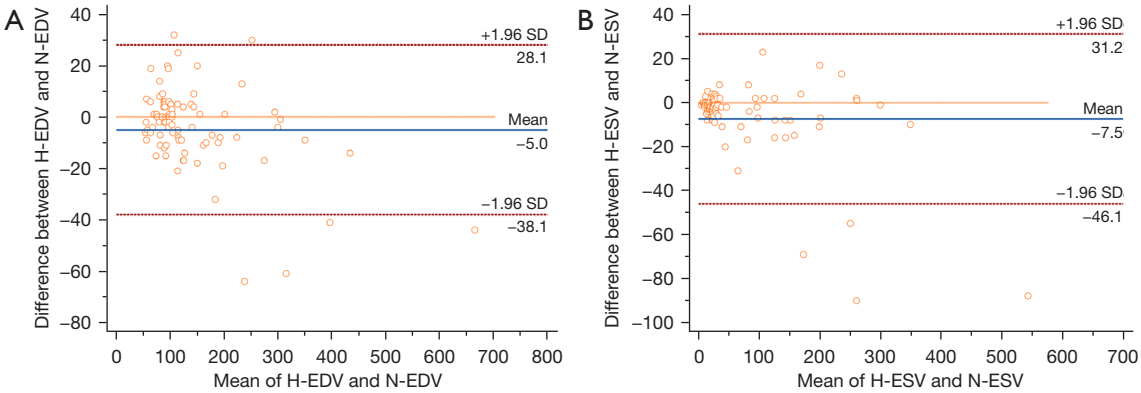

Figure 4 Bland-Altman plots between the arm-down position and the arm-up position for measurement of left ventricular parameters. EDV (A) and ESV (B) were underestimated by a mean of 5.0 (P<0.001) and 7.5 (P<0.001). EDV, end-diastolic volume; ESV, end-systolic volume; H, arm-down position; N, arm-up position.

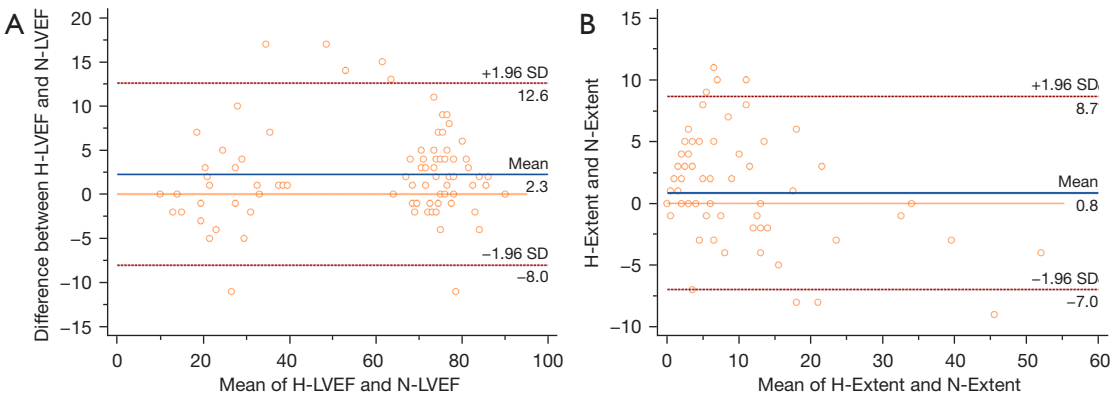

Figure 5 Bland-Altman plots between the arm-down position and the arm-up position for measurement of LV parameters. LVEF (A) and extent (B) were overestimated by a mean of 2.3 (P<0.001) and 0.8 (P=0.02). LV, left ventricular; LVEF, LV ejection fraction; H, arm-down position; N, arm-up position.

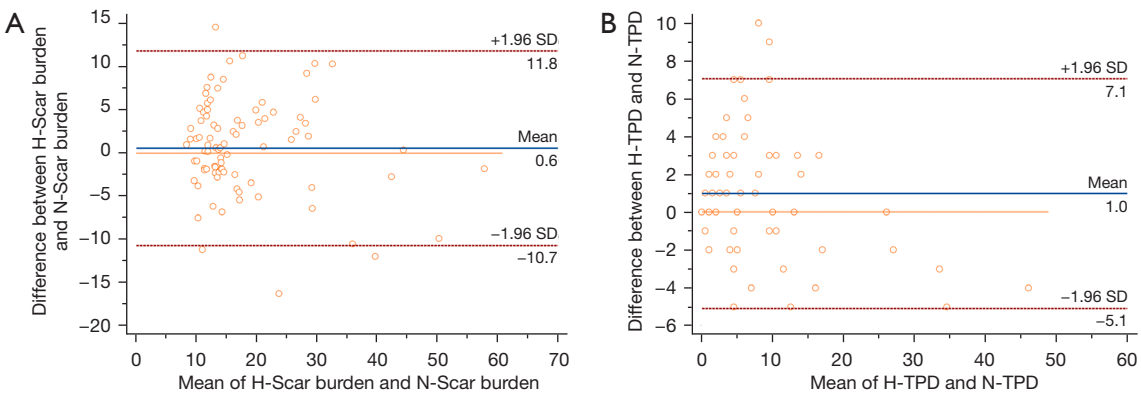

Figure 6 Bland-Altman plots between the arm-down position and the arm-up position for measurement of left ventricular parameters. Scar burden (A) and TPD (B) were overestimated by a mean of 0.6 (P=0.27) and 1.0 (P=0.005). H, arm-down position; N, arm-up position; TPD, total perfusion deficit.

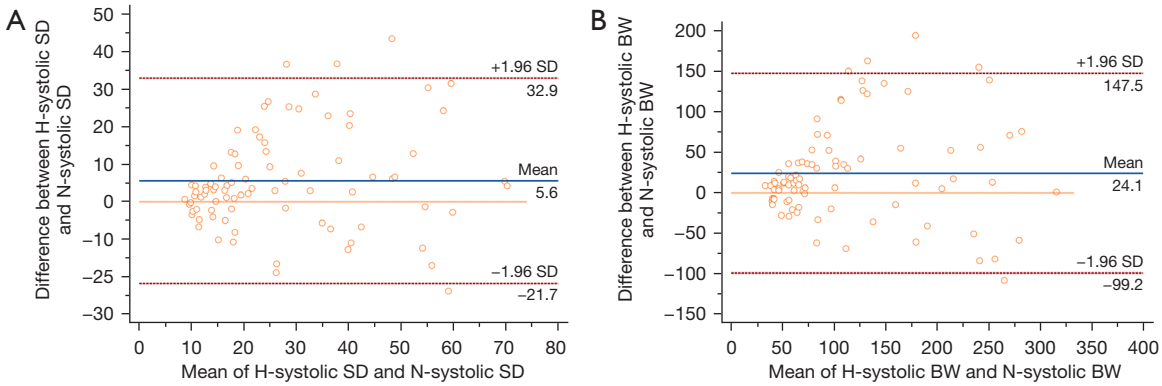

Figure 7 Bland-Altman plots between the arm-down position and the arm-up position for measurement of LV systolic and diastolic dyssynchrony. Systolic SD (A) and systolic BW (B) were overestimated by a mean of 5.6 (P<0.001) and 24.1 (P<0.001). H, arm-down position; N, arm-up position; SD, phase standard deviation; BW, phase histogram bandwidth; LV, left ventricular.

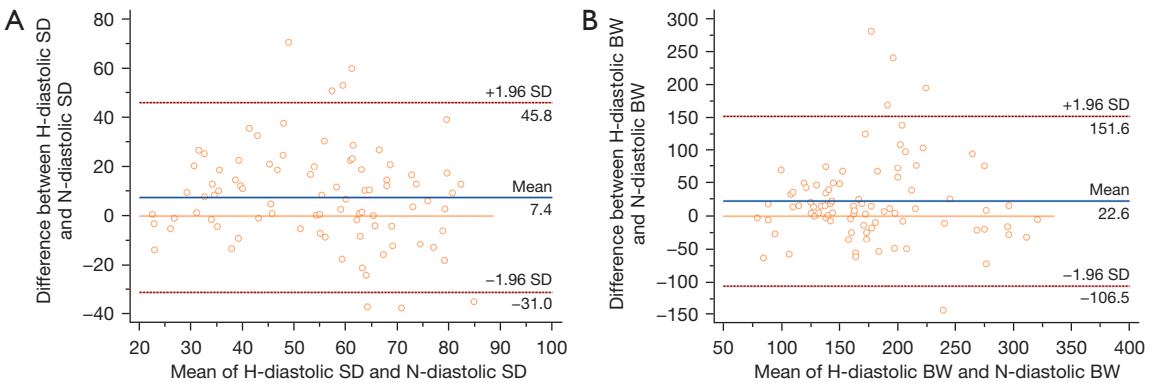

Figure 8 Bland-Altman plots between the arm-down position and the arm-up position for measurement of LV systolic and diastolic dyssynchrony. Diastolic SD (A), and diastolic BW (B) were overestimated by a mean of 7.4 (P<0.001), and 22.6 (P<0.001). H, arm-down position; N, arm-up position; SD, phase standard deviation; BW, phase histogram bandwidth; LV, left ventricular.

could predict clinical outcomes in patients undergoing CRT (21). Phase analysis is a further extension of wall thickening, which is related to the time interval in the 3D LV myocardial wall (9). Phase analysis depends heavily on the myocardial counts at the base of the heart. Therefore, the parameters of phase analysis can be influenced by the heart rate histogram, the gated cine display, and the phase polar map artifact. In our study, the myocardial counts may be partly impaired by the arm, and thus, the LV boundaries cause a mild change in phase analysis. Besides, Kortelainen *et al.* (22) reported that LVMD were sensitive to changes in acquisition time and the increase of noise in myocardial perfusion imaging. Mukherjee *et al.* (23) revealed that low-dose stress images had higher dyssynchrony parameters as compared to high-dose rest images. So, exploring a proper acquisition time and right dosage of radiotracer would be a substantial way to address the influence of arm position in these individuals.

The present research confirms the influence of arm positioning on MPI in different types of heart disease, so physicians should be cautious when applying results from different arm positions. The selection of SPECT combined with CT might be an optional method for minimizing attenuation (24). A preliminary study has demonstrated the potential of utilizing deep learning algorithms for coregistration of attenuation correction maps in MPI (25). Furthermore, artificial intelligence (AI) shows promise for applications in the field of attenuation correction (26). Shi *et al.* (27) developed a deep convolutional neural network that successfully generated accurate attenuation maps to

Table 4 Left ventricular functional parameters in normal groups (n=39) with different arm positions

Variables	Arm-down position	Arm-up position	P value
SRS	1.05±1.64	0.54±1.00	0.037
Extent	2.95±3.48	0.97±1.72	<0.001
Scar burden	13.53±3.60	12.40±3.08	0.115
TPD	3.26±3.04	1.36±1.65	<0.001
EDV (mL)	94.49±24.34	94.54±22.01	0.976
ESV (mL)	23.85±11.31	25.72±12.49	0.006
LVEF (%)	75.67±5.93	73.90±7.73	0.024
Systolic SD	20.36±11.00	14.66±5.20	0.002
Systolic BW	80.31±45.96	55.69±19.38	0.003
Diastolic SD	52.07±19.05	43.48±19.09	0.011
Diastolic BW	157.62±52.94	138.54±45.94	0.071

Data are expressed as mean ± standard deviation. SRS, summed rest score; TPD, total perfusion deficit; EDV, end-diastolic volume; ESV, end-systolic volume; LVEF, left ventricular ejection fraction; SD, phase standard deviation; BW, phase histogram bandwidth.

Table 5 Left ventricular functional parameters in DCM groups (n=52) with different arm positions

Variables	Arm-down position	Arm-up position	P value
SRS	9.88±6.08	10.23±6.25	0.483
Extent	14.15±9.53	14.38±11.44	0.698
Scar burden	26.29±9.49	25.00±11.38	0.185
TPD	11.38±7.16	11.15±8.48	0.584
EDV (mL)	242.50±112.76	255.04±120.87	<0.001
ESV (mL)	183.62±93.97	196.81±109.02	0.002
LVEF (%)	25.54±8.93	24.65±7.89	0.223
Systolic SD	49.41±15.65	41.43±15.03	0.001
Systolic BW	211.62±70.28	180.08±77.90	0.006
Diastolic SD	68.11±12.22	59.48±17.08	0.005
Diastolic BW	239.15±58.52	214.08±70.67	0.028

Data are expressed as mean ± standard deviation. DCM, dilated cardiomyopathy; SRS, summed rest score; TPD, total perfusion deficit; EDV, end-diastolic volume; ESV, end-systolic volume; LVEF, left ventricular ejection fraction; SD, phase standard deviation; BW, phase histogram bandwidth.

Table 6 Left ventricular functional parameters in O-CAD groups (n=32) with different arm positions

Variables	Arm-down position	Arm-up position	P value
SRS	5.63±9.39	5.94±10.33	0.573
Extent	12.44±13.96	11.31±15.55	0.140
Scar burden	18.61±12.32	20.20±13.52	0.01
TPD	10.69±11.76	9.63±13.34	0.098
EDV (mL)	96.44±20.59	96.69±24.60	0.901
ESV (mL)	32.31±25.49	38.25±28.76	0.001
LVEF (%)	69.06±16.57	64.00±16.77	<0.001
Systolic SD	26.99±13.82	25.36±16.13	0.450
Systolic BW	113.00±68.65	102.56±76.76	0.214
Diastolic SD	59.06±13.05	59.29±21.43	0.353
Diastolic BW	186.75±56.49	167.13±54.98	0.018

Data are expressed as mean ± standard deviation. O-CAD, obstructive coronary artery disease; SRS, summed rest score; TPD, total perfusion deficit; EDV, end-diastolic volume; ESV, end-systolic volume; LVEF, left ventricular ejection fraction; SD, phase standard deviation; BW, phase histogram bandwidth.

enhance attenuation correction for SPECT-only scanners. However, further research is required to establish an additional training sample with a validation dataset, which would enable the selection of optimal parameters for model training and the implementation of AI-based algorithms in future studies.

Limitations

Some limitations should be noted in our study. First, the population of our retrospective study was relatively small for establishing a reference range. Second, not all of the patients underwent stress myocardial perfusion SPECT imaging, so the difference between stress and rest imaging is still needed in further studies. Additionally, cardiac magnetic resonance imaging (MRI) or positron emission tomography (PET) was not performed in our study; therefore, the cardiac functional parameters were not compared with other imaging modalities. Finally, more information on the arm position in different software algorithms for G-MPI remains to be determined.

Conclusions

Systolic and diastolic dyssynchrony parameters and most LV functional parameters were significantly influenced by arm position in both normal individuals and HF patients with different pathophysiologies. More attention should be focused on LV dyssynchrony perfusion data during clinical evaluation of CRT implantation procedure.

Acknowledgments

Funding: This work was supported by a grant from the National Nature Science Foundation of China (No. 82100338) and the National Key Research and Development Program of China (Nos. 2022YFC2009700 and 2022YFC2009701).

Footnote

Reporting Checklist: The authors have completed the STROBE reporting checklist. Available at https://qims.amegroups.com/article/view/10.21037/qims-22-1404/rc

Conflicts of Interest: All authors have completed the ICMJE uniform disclosure form (available at https://qims.amegroups.com/article/view/10.21037/qims-22-1404/coif). The authors have no conflicts of interest to declare.

Ethical Statement: The authors are accountable for all aspects of the work in ensuring that questions related to the accuracy or integrity of any part of the work are appropriately investigated and resolved. The study was conducted in accordance with the Declaration of Helsinki (as revised in 2013). The study was approved by the Institutional Ethical Committee of the First Affiliated Hospital of Nanjing Medical University, and informed consent was provided by all the patients.

References

1. Underwood SR, Anagnostopoulos C, Cerqueira M, Ell PJ, Flint EJ, Harbinson M, Kelion AD, Al-Mohammad A, Prvulovich EM, Shaw LJ, Tweddel AC; . Myocardial perfusion scintigraphy: the evidence. Eur J Nucl Med Mol Imaging 2004;31:261-91.
2. Hess PL, Shaw LK, Fudim M, Iskandrian AE, Borges-Neto S. The prognostic value of mechanical left ventricular dyssynchrony defined by phase analysis from gated single-photon emission computed tomography myocardial perfusion imaging among patients with coronary heart disease. J Nucl Cardiol 2017;24:482-90.
3. Ramos SMO, Glavam AP, de Brito ASX, Kubo TTA, Tukamoto G, Sampaio DDCP, de Sá LV. Prone Myocardial Perfusion Imaging and Breast Attenuation: A Phantom Study. Curr Med Imaging Rev 2020;16:70-9.
4. Toma DM, White MP, Mann A, Phillips JM, Pelchat DA, Giri S, Ucrós GR, Heller GV. Influence of arm positioning on rest/stress technetium-99m labeled sestamibi tomographic myocardial perfusion imaging. J Nucl Cardiol 1999;6:163-8.
5. Folks RD, Cooke CD, Garcia EV. Optimizing gated myocardial perfusion imaging processing for phase analysis. J Nucl Cardiol 2016;23:1348-54.
6. Gao Y, Wang YC, Lu CQ, Zeng C, Chang D, Ju S. Correlations between the abdominal fat-related parameters and severity of coronary artery disease assessed by computed tomography. Quant Imaging Med Surg 2018;8:579-87.
7. Elliott P, Andersson B, Arbustini E, Bilinska Z, Cecchi F, Charron P, Dubourg O, Kühl U, Maisch B, McKenna WJ, Monserrat L, Pankuweit S, Rapezzi C, Seferovic P, Tavazzi L, Keren A. Classification of the cardiomyopathies: a position statement from the European Society Of Cardiology Working Group on Myocardial and Pericardial Diseases. Eur Heart J 2008;29:270-6.
8. Chen J, Kalogeropoulos AP, Verdes L, Butler J, Garcia EV. Left-ventricular systolic and diastolic dyssynchrony as assessed by multi-harmonic phase analysis of gated SPECT myocardial perfusion imaging in patients with end-stage renal disease and normal LVEF. J Nucl Cardiol 2011;18:299-308.
9. Chen J, Garcia EV, Folks RD, Cooke CD, Faber TL, Tauxe EL, Iskandrian AE. Onset of left ventricular mechanical contraction as determined by phase analysis of ECG-gated myocardial perfusion SPECT imaging: development of a diagnostic tool for assessment of cardiac

mechanical dyssynchrony. J Nucl Cardiol 2005;12:687-95.
10. Giavarina D. Understanding Bland Altman analysis. Biochem Med (Zagreb) 2015;25:141-51.
11. Nahm FS. Nonparametric statistical tests for the continuous data: the basic concept and the practical use. Korean J Anesthesiol 2016;69:8-14.
12. Malek H, Yaghoobi N, Hedayati R. Artifacts in Quantitative analysis of myocardial perfusion SPECT, using Cedars-Sinai QPS Software. J Nucl Cardiol 2017;24:534-42.
13. Schaefer WM, Lipke CS, Standke D, Kühl HP, Nowak B, Kaiser HJ, Koch KC, Buell U. Quantification of left ventricular volumes and ejection fraction from gated 99mTc-MIBI SPECT: MRI validation and comparison of the Emory Cardiac Tool Box with QGS and 4D-MSPECT. J Nucl Med 2005;46:1256-63.
14. Lecchi M, Martinelli I, Zoccarato O, Maioli C, Lucignani G, Del Sole A. Comparative analysis of full-time, half-time, and quarter-time myocardial ECG-gated SPECT quantification in normal-weight and overweight patients. J Nucl Cardiol 2017;24:876-87.
15. Carrión-Camacho MR, Marín-León I, Molina-Doñoro JM, González-López JR. Safety of Permanent Pacemaker Implantation: A Prospective Study. J Clin Med 2019;8:35.
16. Prvulovich EM, Jarritt PH, Lonn AH, Vorontsova E, Bomanji JB, Ell PJ. Influence of arm positioning on tomographic thallium-201 myocardial perfusion imaging and the effect of attenuation correction. Eur J Nucl Med 2000;27:1349-55.
17. Slomka PJ, Moody JB, Miller RJH, Renaud JM, Ficaro EP, Garcia EV. Quantitative clinical nuclear cardiology, part 2: Evolving/emerging applications. J Nucl Cardiol 2021;28:115-27.
18. Wang C, Shi J, Ge J, Tang H, He Z, Liu Y, Zhao Z, Li C, Gu K, Hou X, Chen M, Zou J, Zhou L, Garcia EV, Li D, Zhou W. Left ventricular systolic and diastolic dyssynchrony to improve cardiac resynchronization therapy response in heart failure patients with dilated cardiomyopathy. J Nucl Cardiol 2021;28:1023-36.
19. Fudim M, Fathallah M, Shaw LK, Liu PR, James O, Samad Z, Piccini JP, Hess PL, Borges-Neto S. The Prognostic Value of Diastolic and Systolic Mechanical Left Ventricular Dyssynchrony Among Patients With Coronary Heart Disease. JACC Cardiovasc Imaging 2019;12:1215-26.
20. Wang C, Tang H, Zhu F, Jiang Z, Shi J, Zhou Y, Garcia EV, Li D, Zhou W. Prognostic value of left-ventricular systolic and diastolic dyssynchrony measured from gated SPECT MPI in patients with dilated cardiomyopathy. J Nucl Cardiol 2020;27:1582-91.
21. Peix A, Karthikeyan G, Massardo T, Kalaivani M, Patel C, Pabon LM, Jiménez-Heffernan A, Alexanderson E, Butt S, Kumar A, Marin V, Mesquita CT, Morozova O, Paez D, Garcia EV. Value of intraventricular dyssynchrony assessment by gated-SPECT myocardial perfusion imaging in the management of heart failure patients undergoing cardiac resynchronization therapy (VISION-CRT). J Nucl Cardiol 2021;28:55-64.
22. Kortelainen MJ, Koivumäki TM, Vauhkonen MJ, Hakulinen MA. Dependence of left ventricular functional parameters on image acquisition time in cardiac-gated myocardial perfusion SPECT. J Nucl Cardiol 2015;22:643-51.
23. Mukherjee A, Singh H, Patel C, Sharma G, Roy A, Naik N. Normal values of cardiac mechanical synchrony parameters using gated myocardial perfusion single-photon emission computed tomography: Impact of population and study protocol. Indian J Nucl Med 2016;31:255-9.
24. Camoni L, Santos A, Attard M, Mada MO, Pietrzak AK, Rac S, Rep S, Terwinghe C, Fragoso Costa P; . Best practice for the nuclear medicine technologist in CT-based attenuation correction and calcium score for nuclear cardiology. Eur J Hybrid Imaging 2020;4:11.
25. Slomka PJ, Miller RJ, Isgum I, Dey D. Application and Translation of Artificial Intelligence to Cardiovascular Imaging in Nuclear Medicine and Noncontrast CT. Semin Nucl Med 2020;50:357-66.
26. Cheng Z, Wen J, Huang G, Yan J. Applications of artificial intelligence in nuclear medicine image generation. Quant Imaging Med Surg 2021;11:2792-822.
27. Shi L, Onofrey JA, Liu H, Liu YH, Liu C. Deep learning-based attenuation map generation for myocardial perfusion SPECT. Eur J Nucl Med Mol Imaging 2020;47:2383-95.

Cite this article as: Zhao Z, Wang C, Peng Z, Bu J, Li C, Li D, Zhou W, Lu R, Tang L, Li Y. The influence of arm positions on mechanical dyssynchrony measured by gated myocardial perfusion imaging. Quant Imaging Med Surg 2023;13(10):6698-6709. doi: 10.21037/qims-22-1404

